

Numerical Analysis of Hollow Cross Section Reinforced Concrete Beams Strengthened by Steel Fibers Under Pure Torsion

Jawad K. Mures^{1,*}, Aqeel H. Chkheiwir², Mazin A. Ahmed³

^{1,2,3} Department of Civil Engineering, College of Engineering, University of Basrah, Basrah, Iraq
E-mail addresses: jawadmures@gmail.com, aqeel.chkheiwir@uobasrah.edu.iq, almazini_engineer@yahoo.com

Received: 11 June 2021; Accepted: 2 August 2021; Published: 5 October 2021

Abstract

This numerical study aimed to investigate the torsional behaviour of hollow cross section reinforced concrete members strengthened with steel fibers (end hooked and corrugated), subjected to pure torsion. The numerical results were compared with experimental results and show good agreement. The experimental study was conducted on ten steel fiber reinforced concrete specimens with low longitudinal reinforcement ratio to investigate the torsional behavior under pure torsion. For this analysis, a computer program (ANSYS 18.2) was used. The brick elements 8-nodes (SOLID65) were used to concrete simulation, while the steel bars simulated as axial members (link 180). The steel fibre was represented theoretically by the stress-strain relationship. The theoretical results indicated that the adopted smeared crack model is capable of making relatively acceptable estimations of cracking and ultimate torsional capacity of the members.

Keywords: Fiber reinforcement concrete, Steel fiber reinforcement, Pure torsion, Hollow cross section members, Mix steel fibers.

© 2021 The Authors. Published by the University of Basrah. Open-access article.

<http://dx.doi.org/10.33971/bjes.21.3.6>

1. Introduction

During the last three decades the non-linear finite element method has become popular for analyze parts of concrete structures. This method has a wide range of useful information from single software program. This information includes strain, displacement, distribution of shear stresses and normal stresses in reinforced concrete members, crack patterns at different load levels, and force in main and lateral steel reinforcement [1]. One of the good-tested programs used to investigate the behavior of actual nonlinear concrete members under pure torsional loads is ANSYS. The ANSYS 18.2 program has the ability of describe and analyze the nonlinear concrete behavior by using a combination of (LINK) and (3D-SOLID) elements in the actual structures [2]. Torsional work is very difficult task in analytical and experimental test as compared to the other types of loads. On the other hand, the experimental tests of pure torsion problems are very hard work as well as the costliness of tests [2]. Therefore, the concrete torsional experimental works are limited in number. The ANSYS 18.2 software program was used for analyzing all modeled beams throughout the present study. The finite element program included modeling the reinforced concrete members, with their dimensions and geometric properties which correspond to the existing experimental results. In ANSYS 18.2, to create the finite element models there are several tasks for the models run property which have to be completed. To reflect the actual physical and mechanical properties of the structure members the elements type and

material geometric properties can be elaborated in the details of specimen.

2. Element types

SOLID65 and LINK180 elements used in modeling the concrete and reinforcement, respectively for concrete beams.

2.1. Idealization of Concrete

ANSYS 18.2 program has the capability for modeling and analyzing different types of materials. Brake element (SOLID65) is used for modeling a 3D solid concrete with or without reinforcement, (SOLID65) has capability of crushing in compression and cracking in tension. The element defines by eight nodes, each node has degrees of freedom in three directions: x , y and z axis. The most important feature of this element is representing of nonlinear material properties. The concrete material has cracking capability in three orthogonal directions, plastic deformations, creep, and crushing. The reinforcing bars elements are capable of compression and tension, but without shear [3]. Figure 1 show the geometrical properties and nodes locations of element (SOLID65).



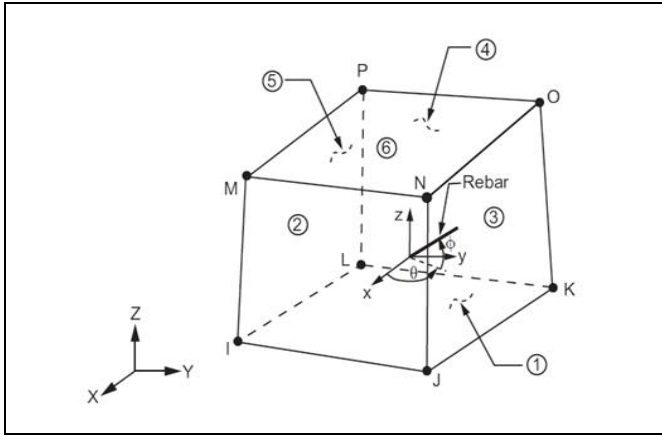


Fig. 1 Element SOLID65-3D [3].

2.2. Idealization of Reinforcement

The finite element models of reinforced bars have generally three alternate techniques that are mainly used for modeling the steel bars in reinforced concrete models: the embedded, the smeared, and the discrete models [4] as shown in Fig. 2. The discrete model Fig. 3, used in the present study to modeling the reinforcement bars as bar or beam elements has two end nodes connected to the nodes mesh of concrete. The steel bars simulated in the same region which is occupied by concrete, full bond between steel bars and surrounding concrete generally assumed. In this study, the longitudinal and transverse reinforcement are modeled by using 2-node discrete element (LINK180).

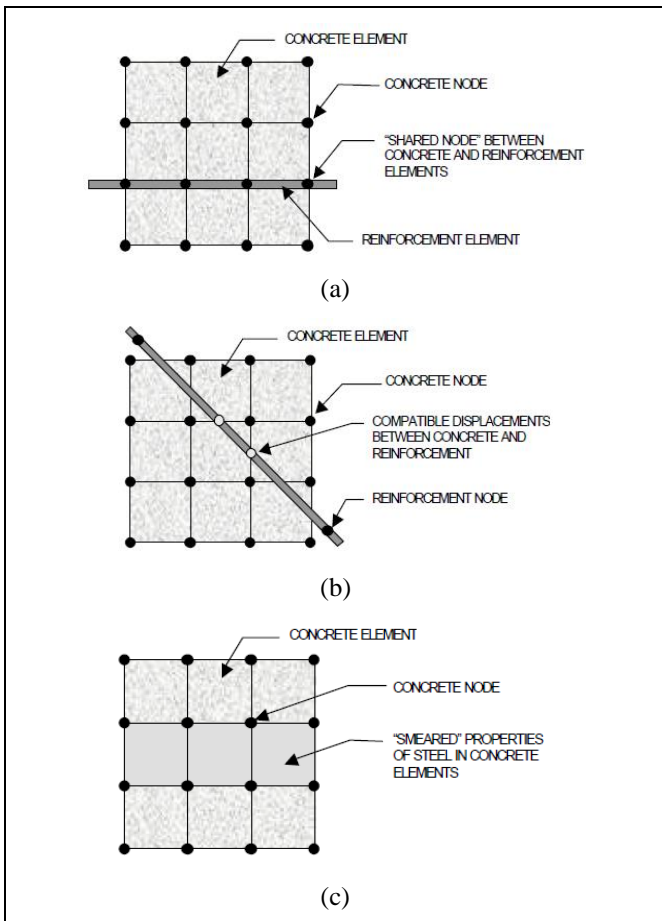


Fig. 2 Models of reinforced concrete: (a) Discrete, (b) Embedded, and (c) Smeared [3].

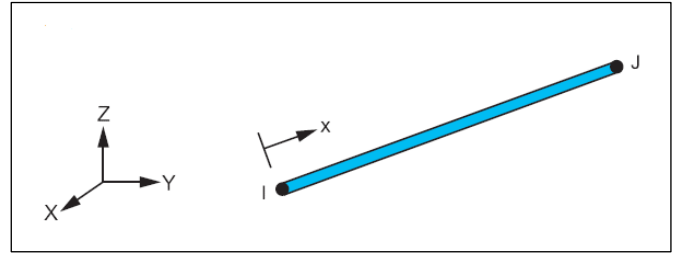


Fig. 3 Element Link 180-3D Spar [3].

3. Experimental work

3.1. Description of Samples

Ten hollow cross section members were tested under pure torsion experimentally, their cross-section dimensions: (250 × 250) mm outer, (150 × 150) mm inner, and (1000) mm long as shown in Fig. 4. Different quantity and types of steel fibers were used in casting the specimens as shown in Table 1. All members were designed to have 4 # 10 mm longitudinal steel bars, and at each end of the beams three # 12 mm closed stirrups were used. To sustain continuity of the members beyond cracking stage, the longitudinal reinforcement percentage was relative higher than the minimum requirement of ACI-Code [5]. Also, the use of steel fibers increases the strength of incomplete members in terms of transverse reinforcement [6]. All materials which used in the experimental study were tested in Thi-Qar University laboratory according to the Iraqi specification requirements No. 45, 1984 [7]. The test results of all materials were in accordance with the above Iraqi specification.

Table 1. Specimen's properties.

Specimen Symbol	Specimen No.	Steel fiber percentage	Steel fibers kind
B 0	1	0 %	No
BE 0.5	1	0.5 %	End hooked
BE 1	1	1 %	End hooked
BE 1.5	1	1.5 %	End hooked
BC 0.5	1	0.5 %	Corrugated
BC 1	1	1 %	Corrugated
BC 1.5	1	1.5 %	Corrugated
BM 0.5	1	0.5 %	Mixed*
BM 1	1	1 %	Mixed*
BM 1.5	1	1.5 %	Mixed*

*Mixed: (50 % corrugated, and 50 % end hooked)

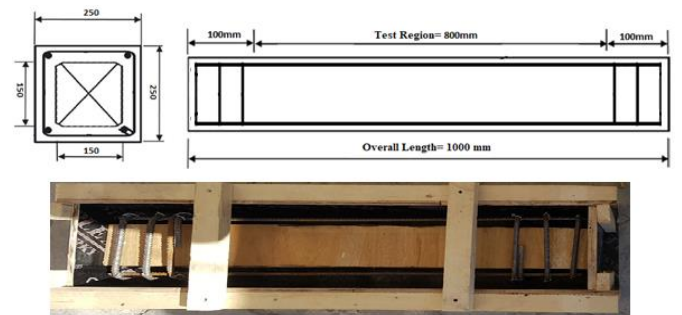


Fig. 4 Geometry of the specimens.

3.2. Concrete Mixing

Several trial mixes were made to achieve the concrete required strengths. The trial mixtures were designed to reach the concrete strengths to 30 MPa at 28 days. The optimum mixture was (1 cement: 2.19 sand: 3 gravel: 0.48 water, by weight). The slump test was about 100 mm. For testing the concrete mix properties, 150 mm cubes, and 100 φ × 300 mm prisms, as shown in Fig. 5 (a) and (b) respectively, prepared for concrete compressive strength, and splitting tensile strength tests, respectively. The compressive strength and tensile strength of optimum mixture were 30.6 MPa and 3.69 MPa respectively.

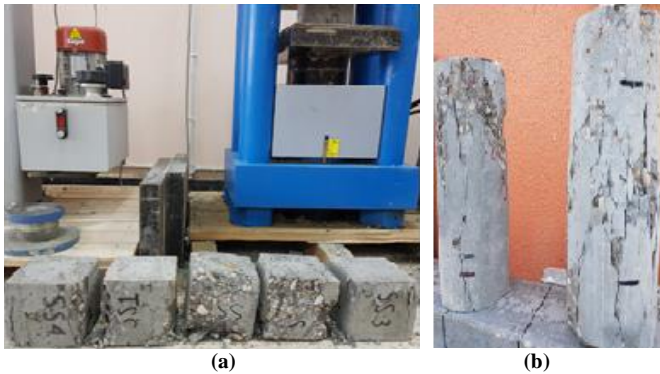


Fig. 5 Concrete mixing properties.

3.3. Testing Procedure

The details of the universal system which used in testing the beams are shown in Fig. 6. The ends of the test beams were clamped with I section steel arms (750 mm), which were loaded through I section steel beam by the universal testing machine to create a pure torsional moment. The supports at each end were placed on roller support to ensure free rotate, extension or contraction during the testing. At both ends of the specimen, electronic angle measures gages were tight to the surface of each beam to measure the twist angle of its ends cross section. The torque is produced by applying a point load to the center of the transmitter I section girder. In order to obtain pure torsion, the girder was used to transfer the concentrated load of the hydraulic testing machine to the ends of the lever arms. The applied load was gradually increased for each 1 kN until the first crack stage. The torsional cracking T_{cr} and the associated twist angle θ_{cr} were recorded, and then the load was applied gradually 5 kN at each step. Readings were recording manually at each load step after first cracking until failure stage were ultimate torsional T_u and failure twist angle θ_f recorded.

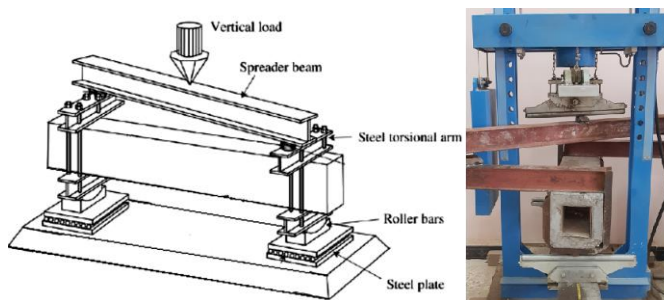


Fig. 6 Test machine.

4. Models of finite element for beam specimens

In this study, the ANSYS 18.2 program was used to modeled and analyzed the beams specimens. Brake element SOLID65 of 8-nodes was used to simulation the concrete, and the LINK180 discrete element of 2-nodes was used to simulation all reinforcement. The main axis of all specimens was coinciding with the z-axis, and the stirrups concedes with direction of x and y axis. As shown in Fig. 7, the torsion load was applied on the two ends of each specimens in opposite directions. The element SOLID65 requires linear and nonlinear isotropic material properties to appropriately concrete models [8], the element material properties were defined by using the experimental data. The coefficient of shear transfer for closed crack (ShrCf-CI), the coefficient of shear transfer for open crack (ShrCf-Op), and Poisson ratio (ν) are listed in Table 2.

Table 2. Model properties of specimens.

Property of Model	Values
ShrCf-CI	0.9
ShrCf-Op	0.6
Concrete Poisson ratio (ν)	0.2
Steel Poisson ratio (ν)	0.3
Steel modulus of elasticity (E_s) (GPa)	200

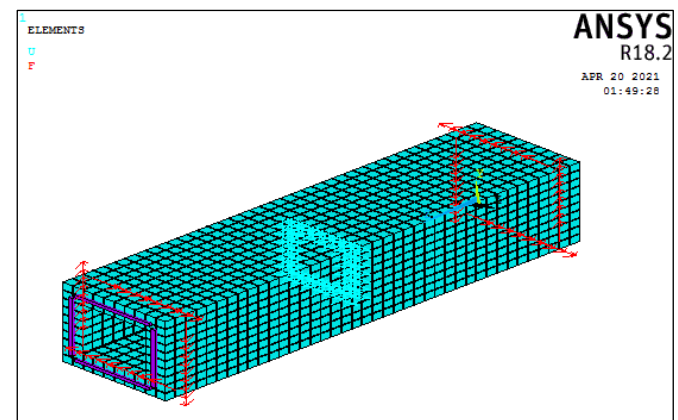


Fig. 7 Finite element model.

4.1. Stress-Strain Relationship for Steel Fibered Concrete

The stress strain curve can be describing the behavior of concrete under uniaxial compressive loads. The slope of the initial region curve represented the concrete modulus of elasticity, and no other part has larger slope. The modulus of elasticity and the stress-strain relationship for end hooked, corrugated, and mix steel fibered concrete under uniaxial compressive stress used in this study was tested experimentally according to ASTM C469-02 [9], by using (150 × 300) mm cylinders concrete. Modulus of elasticity was determined as follows [9]:

$$E_C = \frac{S_2 - S_1}{\epsilon_2 - \epsilon_1} \quad (1)$$

Where:

E_C : Concrete modulus of elasticity (MPa).

S_2 : Stress corresponding to 40 % of ultimate applied loads (MPa).

S_1 : Stress corresponding to a longitudinal strain, $\epsilon_1 = 0.00005$ (MPa).

ϵ_2 : Longitudinal strain produced by stress S_2 .

5. Results of finite element analysis and comparison with experimental results

The numerical analysis results curves of torsion load-twist angle as compared with the experimental results show a good agreement, as shown in Figs. 9 to 11. For comparison purposes the path of loading considered from zero to maximum [10]. This study, show good agreement of comparison between the numerical and the experimental results. Table 3 including the cracking and ultimate torsion load of numerical and experimental results, also the ultimate numerical and experimental twist angle. The first cracking torque of numerical and experimental results for fibred reinforced concrete specimens were compared with ACI-Code data for reinforced concrete members without fiber.

Table 3. Experimental and numerical results.

Specimen symbol	$T_{cracking}$ (Exp.) (kN.m)	$T_{ultimate}$ (Exp.) (kN.m)	$T_{cracking}$ (FEM) (kN.m)	$T_{ultimate}$ (FEM) (kN.m)	$T_{cracking}$ (ACI-Code) (kN.m)	$\theta_{ultimate}$ (FEM) (rad/m)	$\theta_{ultimate}$ (Exp.) (rad/m)
B 0	4.25	6.75	4.2	6.5	4.56	0.011	0.033
BE 0.5	4.65	10.01	5.05	11.05	4.56	0.0271	0.045
BE 1	5.5	12.25	6.5	13.023	4.56	0.035	0.062
BE 1.5	6.4	13.75	7.2	14.55	4.56	0.0347	0.068
BC 0.5	4.45	10.5	5.15	11.25	4.56	0.0271	0.045
BC 1	5.3	11.53	6.45	12.69	4.56	0.035	0.058
BC 1.5	6.1	13	7.25	14.15	4.56	0.0347	0.065
BM 0.5	4.85	9.95	5.1	11.55	4.56	0.0271	0.049
BM 1	5.65	12.73	5.70	12.82	4.56	0.035	0.068
BM 1.5	6.55	14.5	7.28	14.65	4.56	0.0347	0.079

5.1. Crack Patterns

Figure 8 shows the onset of discrete cracks in modeled specimen. The cracks begin to progress as helical shape on all sides. This phenomenon pretended the torsional cracks propagation around the specimen sides. For all models the first and ultimate cracks developing trends along the specimen length were studied. It was observed that, after the first cracking, in the initial cracked zone, the principal stresses and strains increased in all studies specimens. Moreover, the cracks-lines angles conformed approximately quite to the experimental results since it was to be about 45°.

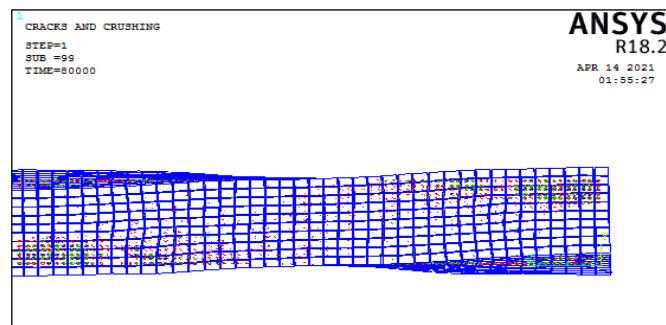


Fig. 8 Crack patterns.

5.2. Load Patterns

The first cracking and ultimate torques of all numerical and experimental specimens were involved in Table 3. It can be observed from this table that the numerical results slightly higher than the experimental. A probable reason of the difference between the numerical and experimental results is due to the perfect bond theoretical assumption between steel bars and surrounding concrete, the relative slipping between the steel fibers and the surrounding concrete, and theoretically, effect of the steel fiber on concrete tensile strength was done through the stress-strain relationship. The results of the ACI-Code are taken constant because of the code equations through which to calculate the cracking and ultimate torque does not take into account the effect of steel fibers (ACI 11. 5. 1). For steel fiber ratios (0.5 %, 1 %, 1.5 %) the percentage of cracking theoretical torque to experimental for end hooked, corrugated and mix steel fiber were: 1.086, 1.18, 1.12, 1.15, 1.21, 1.18, 1.05, 1.01, and 1.11, respectively. Also, for steel fiber ratios (0.5 %, 1 %, 1.5 %) the percentage of ultimate theoretical torque to experimental for end hooked, corrugated and mix steel fiber were: 1.086, 1.098, 1.14, 1.019, 1.12, 1.15, 1.083, 1.04, and 1.04, respectively. The numerical result curves have not the ultimate points of loads and failure points, but have only ultimate load points, because finite element program will stop immediately after the concrete element crushing.

5.3. Effect of Fiber Content

Theoretically the effect of fiber content and its properties were taken into account via the stress-strain relationship. As mentioned previously, the fibred reinforced concrete stress-strain relationship under uniaxial compressive stress used in this study was obtained experimentally. The first cracking and ultimate torque of experimental and numerical results were compared. At high torsional applied load appreciable magnitudes of twist angle were observed shows the torsional ductility of the beams increasing with the increased steel fiber ratio. For all test specimens for steel fiber concrete members with different steel fiber ratios (0.5 %, 1 %, and 1.5 %) give first cracking torque, ultimate torque, and torsional ductility higher than the reinforced concrete members without steel fibers. For the same ratio the mix steel fiber (50 % corrugated and 50 % end hooked) give higher cracking and ultimate torque loads as compared with the two steel fiber types separately. From the obtained results, a great torsional resistance can be obtained by higher percentage of the steel fiber added.

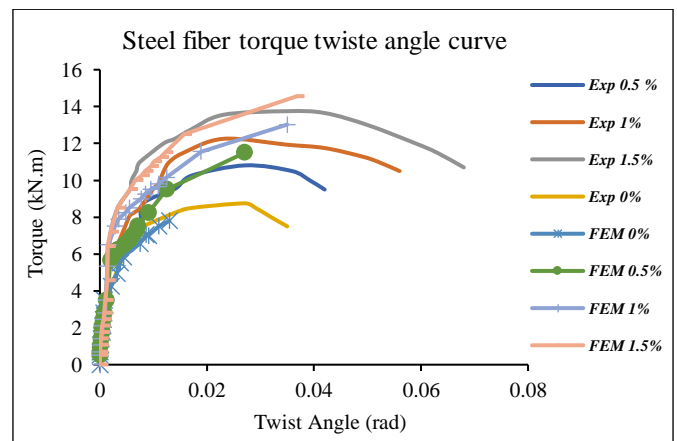


Fig. 9 Relationship of torque-twist angle of end hooked steel fiber.

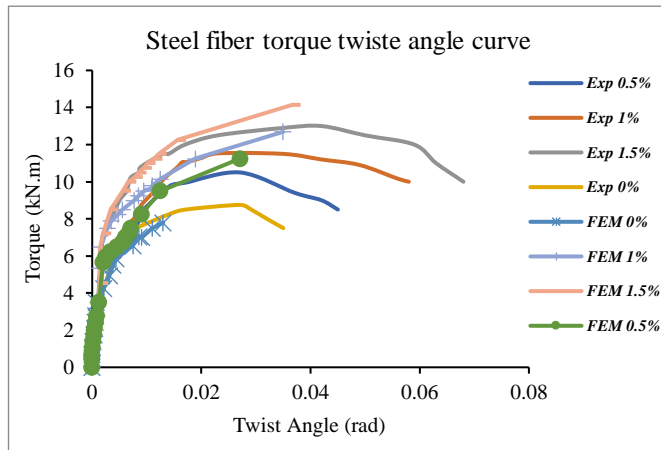


Fig. 10 Relationship of torque-twist angle of corrugated steel fiber.

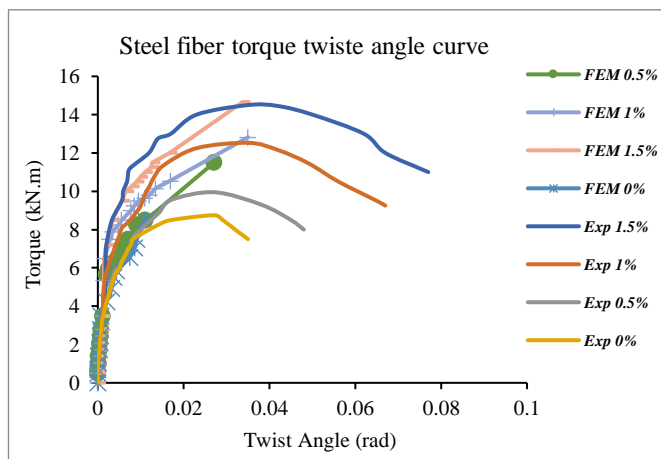


Fig. 11 Relationship of torque-twist angle of Mix steel fiber.

8. Conclusions

1. The first cracking torque and ultimate torque of reinforced concrete structure members under pure torsion will be enhanced with using the steel fibers.
2. The experimental beams were simulated theoretically by using the ANSYS 18.2 software program, and the obtained results were compared. The comparison gives good agreement matched well with the practical results.
3. A probable reason of the difference between the theoretical and experimental results, due to the perfect bond theoretical assumption between steel bars and surrounding concrete, the relative slipping between the steel fibers and the surrounding concrete, and theoretically effect of the steel fiber on tensile strength was done through modifying the stress- strain relationship.
4. The use of corrugated steel fibers has relatively lower torsional resistance than end hooked steel fibers. Also, use of mix steel fibers gives relatively higher torsional resistance than the other two types if used separately.
5. From the curves of the torque-twist angle, notice that the angle of twist of the experimental results was higher values than the angle of twist of numerical. The reason is that the ANSYS program stops analyzing at the maximum applied loads.
6. The used of steel fibers with the concrete mixture enhanced the torsional ductility of concrete members under pure torsion by increasing the angle of twist of strengthened concrete members as compared with the concrete members without fibers.

References

- [1] I. S. I. Harba, "Nonlinear finite element analysis of confined high strength concrete columns under concentric and eccentric loadings", *Journal of Engineering and Development*, Vol. 16, No. 3, pp. 1-18, 2012. <https://www.iasj.net/iasj/download/a861ad75af6d6584>
- [2] T. Tavio and A. Tata, "Predicting nonlinear behavior and stress-strain relationship of rectangular confined reinforced concrete columns with ANSYS", *Civil Engineering Dimension*, Vol. 11, No. 1, pp. 23-31, 2009. <https://ced.petra.ac.id/index.php/civ/article/view/17027>
- [3] ANSYS Inc, "Ansys mechanical APDL element reference", Southpoint, 275 Technology drive, Canonsburg, PA15317, 2018.
- [4] F. A. Tavarez, "Simulation of behavior of composite grid reinforced concrete beams using explicit finite element methods", M.Sc. thesis, Civil Engineering, University of Wisconsin-Madison, 2001.
- [5] ACI Committee 318 Building Code Requirements for Reinforced Concrete, (ACI 318-08), American Concrete Institute, Detroit, 2008.
- [6] S. K. Mohaisen, A. A. Abdulhameed and M. M. Kharnob, "Behavior of Reinforced Concrete Continuous Beams under Pure Torsion", *Journal of Engineering*, Vol. 22, No. 12, pp. 1-15, 2016. <https://joe.uobaghdad.edu.iq/index.php/main/article/view/107>
- [7] Iraqi Specifications IQ.S. No. 45, "Iraqi Standard Specification for Aggregates of Natural Resources used for Concrete and Construction", Central Organization for Standardization and Quality Control, 1984.
- [8] A. J. Wolanski, "Flexural behavior of reinforced and prestressed concrete beams using finite element analysis", M.Sc. thesis, Faculty of the graduate school, Marquette University, 2004. <https://epublications.marquette.edu/theses/4322/>
- [9] ASTM C469-02, "Standard Test Method for Static Modulus of Elasticity and Poisson's Ratio of Concrete in Compression", Vol. 4.2, pp. 1-5, 2002. <https://doi.org/10.1520/C0469-02>
- [10] D. Mostofinejad and S. B. Talaeitaba, "Nonlinear Modeling of RC Beams Subjected to Torsion using the Smeared Crack Model", Elsevier, *Procedia Engineering*, Vol. 14, pp.1447-1454, 2011. <https://doi.org/10.1016/j.proeng.2011.07.182>
- [11] I. A. S. Al-Shaarbaf, A. N. Attiyah, and M. S. Shuber, "Non-linear Finite Element Analysis of Prestressed Concrete Member under Torsion", *Kufa Journal of Engineering*, Vol. 4, No. 2, pp. 29-51, 2013.